The Maximum Circular Velocity Dependence of Halo Clustering

Contents

1 Introduction

The halo model provides a connection between dark matter halos and galaxies, and it has been remarkably successful in describing observations of galaxy clustering. In particular, the Halo Occupation Distribution (HOD) and the Conditional Luminosity Function (CLF) are the two most widely used models of the galaxy-halo connection. In order to populate halos with galaxies, the HOD gives the probability $P(N|M)$ that a halo with mass M hosts N galaxies, while the CLF models the mean abundance $\Phi(L|M)$ of galaxies with luminosity L which live in a dark matter halo of mass M. Those two models are convertible that we can obtain an HOD by integrating the CLF against luminosity and a CLF by differentiating the HOD with respect to luminosity. The fundamental assumption in both formalisms is that galaxy occupation statistics are characterized entirely by halo mass.

Some studies show that the most important halo property that influences the properties of galaxies within halos is halo mass [White and Rees, 1978 and one more]. This is often extended to halo abundance and halo clustering as an assumption that halo mass is the most influential halo property to characterize its abundance and clustering. The motivation behind this assumption comes from the simple excursion set formalism, which models halo assembly and clustering from the random walks of the density fluctuation. This formalism often assumes that halo environment and halo assembly history have no correlation.

The halo clustering in N-body simulations, however, exhibits dependence on halo mass as well as on additional properties such as halo formation time [XXX]. The dependence of halo clustering upon other properties besides halo mass is known as halo assembly bias. There have been several studies showing the correlation between halo formation time and environment, and therefore any other properties that depend on formation time or environment (such as concentration, spin, and velocity anisotropy) affect to the assembly bias. If the galaxy properties in halos correlate with halo environment, it implies that the galaxy occupation statistics also correlate with halo assembly bias. Several groups study the correlation between galaxy formation and halo assembly bias both theoretically (Croton et al. 2007) and observationally (XXX). Even though semi-analytic approach shows the significant influence of halo assembly bias on galaxy clustering, there have been mixed responses to the detection of such a correlation observationally.

As a response to halo assembly bias, a recent trend in connecting halos and galaxies has been to use the Abundance Matching technique based on the maximum circular velocities of halos. This is because assembly bias is a generic prediction in this technique. The general idea behind the Abundance Matching technique is that the size of halos and the size of galaxies are tightly correlated in a monotonic manner so that one can assign the largest galaxy to the largest halo and so on. For the size of galaxies, the luminosity or stellar mass of galaxies is often chosen, while the maximum

circular velocity is often used as a measure of halo size. The motivation behind use of the maximum circular velocity is that it is a proxy for the potential well depth of halos and depends only on the central part of the halo potential (i.e., potentially more closely related to galaxy formation).

Talk about Backsplash halos and the related researches.

In this paper, we explore the dependence of galaxy clustering on the central velocity dispersion both on small and large scales. We show that some of the features on small scales in a detailed halo model come from the effects of back-splash halos, which is one of the categories of halos classified based on the halo merger tree.

## 2 The Simulation: Read Zentner 2013 and Fill what I need to write

We use cosmological N-body simulations called the Bolshoi simulation [XXX:http://arxiv.org/abs/1002.3660 (Klypin, Trujillo-Gomez, and Primack, 2011)] and the MultiDark simulation [XXX: http://arxiv.org/abs/1109.0003 (Riebe et al., 2012), Prada et al. 2011] to investigate the maximum circular velocity dependence of halo clustering. We use both simulations in order to obtain a large dynamic mass range. Both simulations assume a flat ΛCDM model with density parameters $\Omega_m = 0.27$, $\Omega_\Lambda = 0.73$, $\Omega_b = 0.0469$, and $\sigma_8 = 0.82$, $n = 0.95$, $h = 0.70$. The Bolshoi simulation uses 2048^3 particles in a periodic box with side length $250h^{-1}$Mpc. The mass of each particle is $1.35 \times 10^8 h^{-1}$M$_\odot$ with the force resolution $1h^{-1}$kpc. The MultiDark simulation uses 2048^3 particles in a periodic box with side length $1000h^{-1}$Mpc. The mass of each particle is $8.721 \times 10^9 h^{-1}$M$_\odot$ with the force resolution $7h^{-1}$kpc. The simulations were run with the Adaptive Refinement Tree Code [ART: Kravtsov et al. 1997, Gottloeber & Klypin 2008]. Halo catalogues and snapshots for dark matter particles are available at http://www.multidark.org.

We use halo catalogues generated by the ROCKSTAR, which is a phase-space, temporal halo finder [XXX]. The ROCKSTAR identifies halos and subhalos down to the maximum circular velocity $V_{\max} \sim 55$km/s and also provides merger trees. Those catalogues are publicly available at http://hipacc.ucsc.edu/Bolshoi/MergerTrees.html.

Based on the halo catalogue, we classify halos into three different categories: host halo, subhalos, and ejected halos. Host halos are the halos that have never been within the virial radius of more massive halos. Subhalos are the halos which are within the virial radius of more massive halos at $z = 0$. Ejected halos, sometimes called "backsplash" halos, are the distinct halos at $z = 0$ whose main progenitors passed through the virial radius of a more massive halos at least once in the past. In order to identify ejected halos, we build a merger tree by using a merger tree algorithm CONSISTENT TREES[cite]. In later sections, when we say halos without any specifications, we include both host halos and ejected halos.

The dark matter halos in the halo catalogue at $z = 0$ are defined to be spherical regions whose average density equal to $\Delta_{\mathrm{h}}\rho_{\mathrm{crit}}$ where $\Delta_{\mathrm{h}} = 360$ at $z = 0$ according to Bryan & Norman fitting function [XXX] and whose radius R_{vir} corresponds to $M_{\mathrm{vir}} = 4\pi\Omega_m\rho_{\mathrm{crit}}\Delta_{\mathrm{h}}R_{\mathrm{vir}}^3/3$. The value $\Delta_{\mathrm{h}} = 360$ is used to define virial mass for the ΛCDM cosmology. Note that even though subhalos are distinct and bound objects within the host halos, the masses and radii of subhalos do not follow the above virial definition, because their structures are strongly affected by the potentials of their host halos. In order to define the maximum circular velocity for each halo, the average velocity of the particles (or $\sqrt{\mathrm{GM}(r)/r}$) within the radius r is repeatedly computed with increasing r until r reaches to R_{vir}.

For the sake of the internal structure of halos to be resolved well enough, we made a conservative cut in mass and maximum circular velocity. We use halos whose mass is greater than $10^{12}h^{-1}$M$_\odot$ (corresponding to > 100 particles per halo) and whose maximum circular velocity is greater than 200km/s for the MultiDark simulation, and halos whose mass is greater than $10^{11}h^{-1}$M$_\odot$ (corresponding to > 740 particles per halo) and whose maximum circular velocity is greater than 95km/s for the Bolshoi simulation. Those values correspond to the peak in the number of halos by binning them as a function of mass and maximum circular velocity. The halos which have smaller masses or maximum circular velocities are not considered to be complete based on the predictions for halo mass functions, which are a monotonically increasing function with the decrease in halo mass. As we will see in Section 3, simultaneous dependence of halo clustering on M_{vir} and $V_{\max}$, the cut is not enough. But all the results pass this cut unless it is noted.
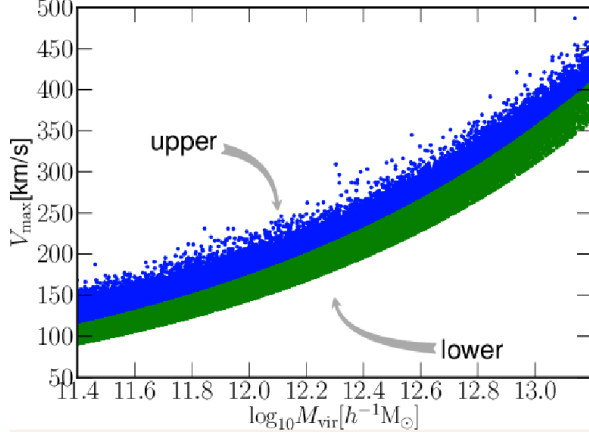
Figure 1. Distribution of halo mass and maximum circular velocity at $z = 0.0$ for halos from the Bolshoi simulation. The blue dots represent halos whose observed maximum circular velocity, $V_{max,obs}$, is greater than $\overline{V}_{max}$, while the green dots are the ones with smaller $V_{max,obs}$ than $\overline{V}_{max}$. The boundary between blue and green dots correspond to $\overline{V}_{max}$ computed from Eq. 3.1.

3   The Maximum Circular Velocity Dependence of Halo Clustering

In this section, we investigate the maximum circular velocity dependence of halo clustering on both large and small scales. We first start with an analytic expression of the maximum circular velocity computed from the halo mass and its concentration. Then, we explain how we select halos for each sample to remove the halo mass dependence using the analytic expression of the maximum circular velocity. Finally, we show how halo biases differ for those samples both on large scales and small scales.

3.1   The Maximum Circular Velocity

In order to compute the maximum circular velocity for halos, we assume that dark matter halos are defined as a spherical halo with a virial radius. Those halos have average density equal to $\Delta_h \rho_{crit}$ where $\Delta_h = 360$ for $z = 0$ according to Bryan & Norman fitting function [XXX]. We also assume that those spherical halos have an NFW density profile (XXX). Then, the maximum circular velocity $\overline{V}_{max}$ as a function of the halo mass M_{vir} and its concentration c is given by:

$$\overline{V}_{max} = 0.465 M_{vir}^{1/3} \sqrt{G(\frac{4}{3}\pi \Delta_h \rho_{crit} \Omega_m)^{1/3} \frac{c}{\ln(1+c) - c/(1+c)}}. \tag{3.1}$$

The median concentration-mass relation at $z = 0$ obtained from the Bolshoi simulation in Ref. XXX(Klypin et al. 2011) is:

$$\log_{10} c = -0.097 \log_{10} M_{vir} + 2.148. \tag{3.2}$$

By using the above median concentration to Eq. 3.1, we obtain a one to one mapping between the virial halo mass and its maximum circular velocity, denoted as $\overline{V}_{max}$ hereafter. Given this mapping, we can translate clustering measurements as a function of halo mass into predicted clustering measurements as a function of maximum circular velocity. Our goal below is to determine whether this conversion describes the measured clustering or if there is a residual dependence on the maximum circular velocity.

3.2   Samples

To begin with, we split the sample of halos described in Section 2 into a sequence of virial mass bins, chosen such that there are the same numbers of halos in each bin. This process is reminiscent of an abundance matching procedure (cite XXX). We then further split each bin into two subsamples with their observed $V_{max,obs}$ greater than (denoted by "upper") or less than (denoted as "lower") $\overline{V}_{max}$.

Fig. 1 shows the distribution of halo mass and maximum circular velocity classified into "upper" (blue dots) and "lower" (green dots) samples as an example. Note that the number of halos in "upper" and "lower" subsamples are almost equal for any halo mass bins. This selection ensures that both the upper and lower subsamples have the same mean halo mass. Therefore, in the absence of an additional M_{vir} dependence on clustering, these samples should have the same clustering properties. Note that this would not be true if we had simply split the sample along V_{max}, since the two resulting subsamples would have different mean halo masses.

3.3 Halo Bias

In order to measure halo biases, we first compute halo-matter cross correlation functions for each subsample. We used cross correlation functions to reduce the shot noise effect on the error. Here, instead of using full DM particles, we subsample 10^6 particles to compute the cross correlation functions and matter auto correlation functions. Then, we define a linear bias:

$$b_{\mathrm{lin}} = \sum_i (\xi_{hm}(r_i)/\xi_{mm}(r_i))/N_{\mathrm{bin}}, \tag{3.3}$$

where ξ_{hm} and ξ_{mm} are halo-matter and matter-matter correlation functions and we take the average of the ratio on r from $10h^{-1}$Mpc to $20h^{-1}$Mpc, which contains 20 bins in total.

Fig. 2 shows linear biases as a function of halo mass by splitting each sample into "upper" and "lower" subsamples. For large halo masses, the "lower" subsamples have larger linear biases than the "upper" subsamples. This result is consistent with the result discussed in Ref. XXX(Dalal et al. 2008). For low halo masses, the "upper" subsamples have larger linear biases than the "lower" subsamples. Those halos, which have larger maximum circular velocities than $\overline{V}_{\mathrm{max}}$, are the ones which are supposed to grow into larger mass halos, but somehow the mass growth is suppressed due to a tidal field [XXX: Wang et al.]. This is why those halos in the "upper" subsamples cluster more strongly than the ones in the "lower" subsamples. As halo mass decreases, the difference in linear bias between the "upper" and "lower" subsamples increases up to $\sim 40\%$. On the low mass end, there is a drop in the ratio of the linear biases. We think that the drop is due to mass resolution of the simulation.

Although halo biases are constant on large scales, halo biases on small scales are scale-dependent (XXX:reference). We explore whether the "upper" and "lower" subsamples have different scale-dependence in small scale halo biases. In order to explore this, we take the ratio of the cross correlation functions between the "upper" and "lower" subsamples and normalize it with their linear biases. Fig. 3 shows the ratios for several mass bins. The first three mass bins labeled in the figure, $\log_{10}\mathrm{M}[\mathrm{h}^{-1}\mathrm{M}_\odot] = 11.7, 12.0, 12.2$, are from the Bolshoi simulation, and the last two mass bins, $\log_{10}\mathrm{M}[\mathrm{h}^{-1}\mathrm{M}_\odot] = 12.7, 13.1$, are from the MultiDark simulation. The "upper" and "lower" subsamples have very different scale-dependence, especially around 1 to $2h^{-1}$Mpc. Furthermore, the difference on small scales becomes larger for lower halo mass samples. This implies that those low mass halos in the "upper" subsamples cluster strongly and are likely to live in hot environments near massive halos.

Up until present, we have used both host halos and ejected halos to compute halo biases. Both types of halos are identified as distinct halos at $z = 0$. Ejected halos, however, are halos which were identified as part of more massive halos at one or more occasions in the past, but were ejected and now exist at a host halo at $z = 0$. Those ejected halos tend to exist around more massive halos (any reference?), and only some of them may be gravitationally bound to other more massive halos. Therefore, the effect on scale-dependent biases may be caused by those ejected halos. To test this, we compute halo-matter cross correlation functions without the ejected halos. Similar to Fig. 2, we first compare linear biases as a function of halo mass. We observe that the ratios of linear biases between the "upper" and "lower" subsamples are suppressed by $\sim 10\%$. Next, we compare cross correlation functions on small scales, as shown in Fig. 4, similar to what was done in Fig. 3. Fig. 4 only shows the results for low mass halos from the Bolshoi simulation. This is because we do not find many ejected halos in the MultiDark simulation due to its mass resolution. Once the ejected halos
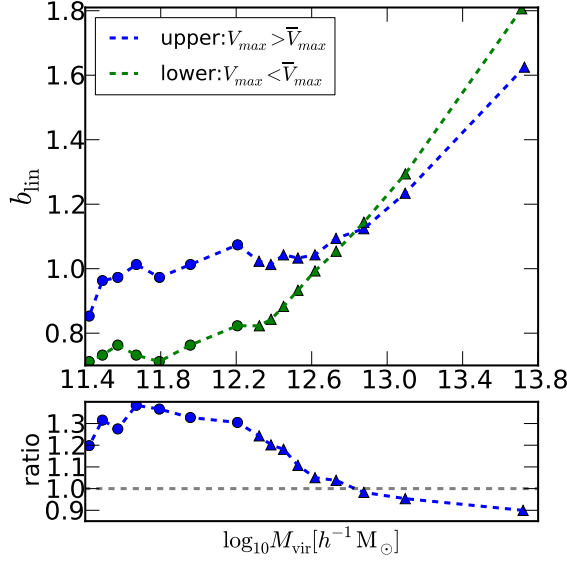
Figure 2. Upper panel: Linear bias at $z = 0.0$ as a function of halo mass from the Bolshoi simulation (circle points) and the MultiDark simulation (triangle points). The blue circles correspond to a linear bias for halos whose maximum circular velocities are greater than $\overline{V}_{\max}$ (called "upper" samples in the text), while the green circles correspond to halos whose maximum circular velocities are smaller than $\overline{V}_{\max}$ (called "lower" samples). Lower panel: Ratio of linear biases between "upper" (i.e., $V_{\max} > \overline{V}_{\max}$) and "lower" (i.e., $V_{\max} < \overline{V}_{\max}$) samples from the Bolshoi simulation and the MultiDark simulation. As halo masses decrease, the difference on linear bias between "upper" and "lower" samples becomes larger up to 40%. .

have been removed, the deviation of the halo bias on small scales is greatly reduced. This implies an intimate connection between assembly bias and subhalo back-splashing.

We conclude that halos which have different $V_{\max}$ cluster differently even when those halos have the same virial mass. In particular, the scale-dependence of halo biases on small scales is significantly different, which is mainly caused by the ejected halos.
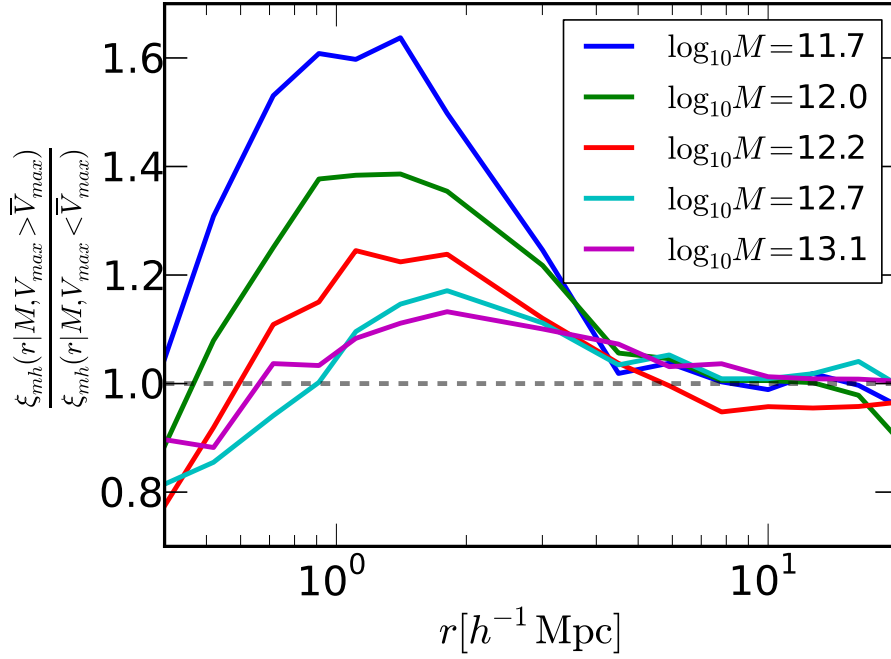
Figure 3. Ratio of halo-matter cross correlation functions between "upper" and "lower" subsamples normalized by their linear biases. The plots are from the Bolshoi simulation and the MultiDark simulation at $z = 0$. Each line corresponds to different halo mass bins labeled in the plots. The top three lines that correspond to low mass halos are computed from halos in the Bolshoi simulation, while the bottom lines are from the Multi-Dark simulation. Those plots show that "upper" and "lower" subsamples have different scale-dependence on small scales and the relative scale-dependence between those subsamples increases smoothly with decreasing halo mass.
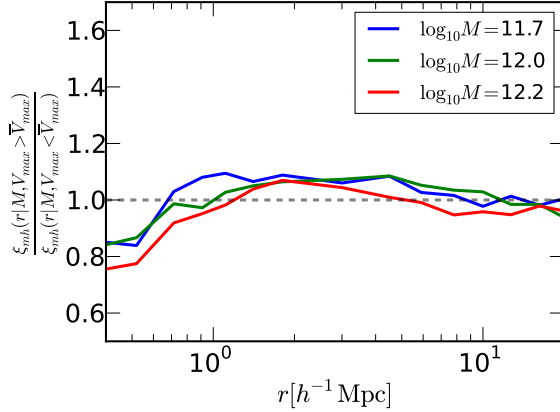
Figure 4. The same figures as Fig. 3 without ejected halos only from the Bolshoi simulation. As can be seen by comparing these results to those in Fig. 3, the V_{max}-dependence of halo bias on small scales is dramatically reduced by excluding ejected subhalos. This implies an intimate connection between assembly bias and subhalo back-splashing.

–use jackknife sampling to put error bars

4   Applications

In this section, we demonstrate possible observational relevances of the results in the previous section to complement the halo theory results. We start with the abundance matching (citation?) technique based on halo mass and the maximum circular velocity, and then compute $\Delta\Sigma(\mathrm{R})$ using those two different abundance matching technique.

4.1   Mvir-based v.s. Vmax-based

In abundance matching, we link galaxy populations to halo populations by assuming that big galaxies live in big halos in a hierarchical manner. The question is what "big" halos really means. To rank order halos, we want to identify what kind of physical properties characterize halo "size". As a first step, we explore how the abundance matching based on halo mass and maximum circular velocity influence halo clustering.

Similar to the previous section, we compute halo-matter cross correlation functions for the abundance matched samples by splitting halos into a sequence of halo mass bins, $\overline{n}(M_{\mathrm{vir}})$, and the maximum circular velocity bins, $\overline{n}(V_{\mathrm{max}})$, chosen such that each bin has the same number of halos. We observe that when we include ejected halos, the linear biases for the V_{max}-samples are larger than the ones for the M_{vir}-samples by 5%, while the difference in linear biases is suppressed to 2% by excluding ejected halos. This result is consistent with the result in Sec. 3.2. The magnitude of the difference, however, is smaller than the cases of splitting the samples based on $\overline{V}_{\mathrm{max}}$.

We also compare the cross correlation functions on small scales. Figure 5 displays data in the same way as Figure 3 with the ejected halos on the left and without the ejected halos on the right. When those samples contain ejected halos, the V_{max}-samples show very different scale-dependence on halo bias than the M_{vir}-samples do. This scale-dependent feature becomes stronger as halo mass decreases. Without ejected halos, the difference on small-scale biases between the M_{vir}- and V_{max}-samples is reduced to $\sim 5\%$, which is the same order of magnitude as the case of Sec. 3.3 shown in Fig. 4.
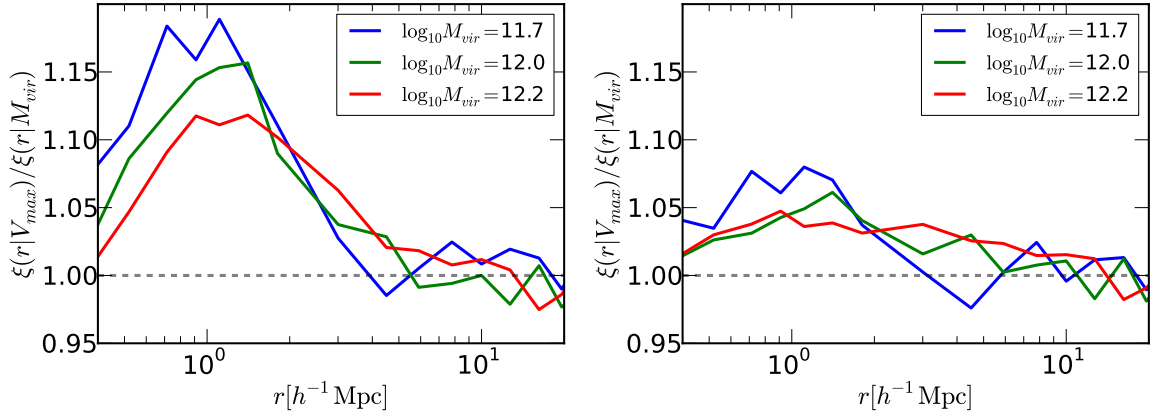
Figure 5. Ratio of halo-matter cross correlation functions between M_{vir}-based and V_{max}-based abundance matching samples with ejected halos (left) and without ejected halos (right). The ratios are normalized by their linear biases. Each line corresponds to different halo mass bins labeled in the plots. With ejected halos, the halo biases computed from the V_{max}-samples have very different scale-dependence than the ones from the M_{vir}-samples. By removing those ejected halos, the difference is more or less removed.

4.2 $\Delta\Sigma(r)$

–Select a bin of Milky Way mass host halos, and select their number-density-matched Vmax-selected equivalent. Use Peter Behroozi's stellar-to-halo mass relation to estimate the stellar mass of the central galaxy that would be found in these halos, then plot the halo-matter cross-correlation as a function of scale, over-plotting the two results.

–want to show: We show that the galaxy-galaxy lensing signal of low-mass centrals is impacted at the xxx-yyy% level, in a highly scale-dependent fashion, by the theoretical choice to empirically connect stellar mass to either host halo Vmax or Mvir.

5   Discussion

Previous studies show the dependencies of halo clustering on other parameters besides halo mass and how those dependencies affect on observations.

We explore the dependency of clustering on the maximum circular velocity and how it makes defference on observations.

We find that halo clustering depends on the maximum circular velocity both on large and small scales. Our finding for the clustering on large scales is consistent with the result in Dalal et al. 2008.The dependence of the clustering on small scales is mostly due to backsplash halos. This is first time to show how the backsplash halos affect the clustering on small scales. It suggests that the backsplash halos should be treated as subhalos and not as host halos.

The limitations of my study is that we did not investigate whether those backsplash halos are actually gravitationally bound to more massive halos which are close to those backsplash halos. Also, at this point, we are not sure whether all backsplash halos should be treated as subhalos or some subclasses of backsplash halos are subhalos.

In conclusion, XXX.